Expression signatures of the lipid-based Akt inhibitors phosphatidylinositol ether lipid analogues (PIAs) in NSCLC cells

Chunyu Zhang[1], **Abdel G. Elkahloun**[2], **Hongling Liao**[3], **Shannon Delaney**[1], **Barbara Saber**[1], **Betsy Morrow**[1], **Joell J. Gills**[1], **M. Christine Hollander**[1], **George C. Prendergast**[4], and **Phillip A. Dennis**[1,*]

[1] Medical Oncology Branch, Center for Cancer Research, NCI, Bethesda, MD 20892

[2] Cancer Genetics Branch, NHGRI, NIH, Bethesda, MD 20892

[3] Sequencing Facility, SAIC-Frederick, NCI at Frederick, Gaithersburg, MD 20877

[4] Lankenau Institute for Medical Research, Wynnewood, PA 19096

Abstract

Activation of the serine/threonine kinase Akt contributes to the formation, maintenance, and therapeutic resistance of cancer, which is driving development of compounds that inhibit Akt. Phosphatidylinositol ether lipid analogues (PIAs) are analogues of the products of PI3K that inhibit Akt activation, translocation, and the proliferation of a broad spectrum of cancer cell types. To gain insight into the mechanism of PIAs, time-dependent transcriptional profiling of 5 active PIAs and the PI3K inhibitor LY294002 (LY) was performed in NSCLC cells using high-density oligonucleotide arrays. Gene ontology analysis revealed genes involved in apoptosis, wounding response, and angiogenesis were upregulated by PIAs, while genes involved in DNA replication, repair and mitosis were suppressed. Genes that exhibited early differential expression were partitioned into 3 groups; those induced by PIAs only (DUSP1, KLF6, CENTD2, BHLHB2, PREX1), those commonly induced by PIAs and LY (TRIB1, KLF2, RHOB and CDKN1A), and those commonly suppressed by PIAs and LY (IGFBP3, PCNA, PRIM1, MCM3 and HSPA1B). Increased expression of the tumor suppressors RHOB (RhoB), KLF6 (COPEB) and CDKN1A (p21Cip1/Waf1) was validated as an Akt-independent effect that contributed to PIA-induced cytotoxicity. Despite some overlap with LY, active PIAs have a distinct expression signature that contributes to their enhanced cytotoxicity.

Keywords

Akt; microarray; PIA; RhoB; NSCLC

Introduction

The PI3K/Akt/mTOR pathway is a promising target in cancer since its activation promotes cellular growth, survival and contributes to tumorigenesis *in vivo*, while inhibition of the pathway promotes apoptosis in cancer cells and increases responsiveness to chemotherapy or radiation (1–5). Akt has an important role in lung cancer since it is activated in response to tobacco components in vitro (6, 7), and the phenotypic progression of tobacco

*To whom correspondence should be addressed: 37 Convent Dr., Rm. 1118B, Bethesda, MD 20892, USA Phone: (301)-496-0929. Fax: (301)-435-4345. dennisp@mail.nih.gov.

carcinogen-induced lung lesions is dependent upon activation of Akt and mTOR (8, 9). In NSCLC, Akt activation is specific for tumor tissues vs. surrounding normal lung tissues and confers a poor prognosis (10). Despite the strong rationale to target Akt, however, few Akt inhibitors exist.

To address this need, we used molecular modeling to synthesize structurally modified phosphatidylinositol ether lipid analogues (PIAs) designed to interfere with the pleckstrin homology (PH) domain of Akt (11). Five PIAs were identified that rapidly inhibited Akt activation, as well as the phosphorylation of multiple downstream substrates without affecting kinases upstream of Akt (12). PIAs selectively induced apoptosis in NSCLC and breast cancer cell lines with high endogenous levels of Akt activation. Although the PIAs appeared interchangeable in their abilities to inhibit Akt and cause cell death, they induced more cell death than an established PI3K inhibitor, LY294002, despite similar inhibition of the Akt pathway, which suggests PIAs might have additional targets. Support for this hypothesis came from studies of PIAs in the NCI60 cell line panel where activity of PIAs correlated with levels of phosphorylated but not total Akt, but other targets with higher correlation coefficients were identified (13).

Microarrays have been used to query transcriptional programs that underlie processes relevant to cancer such as proliferation (14), transformation (15), senescence (16), metastasis (17), epithelial to mesenchymal transition (18) and activation of oncogenic pathways (19). Elucidation of these programs is important to the development of new therapies. For example, transcriptional profiling of normal vs. tumor tissues has led to the identification of new targets and pharmacodynamic biomarkers to predict efficacy and clinical outcome (20, 21). Profiling of drug-induced gene transcription has been used to uncover the mechanism of action of novel agents, elucidate structure activity relationships, and to determine on-target vs. off-target effects (22, 23).

To elucidate transcriptional changes that could mediate the cytotoxic activity of PIAs, expression profiling in NSCLC cells was performed. We segregated changes in gene expression that were shared by both PIAs and LY294002 and therefore likely due to effects on the PI3K/Akt pathway, from those that were unique to PIAs and therefore might be considered "off-target" effects. Although greatly overlapping with LY294002 in suppression of cell cycle genes, active PIAs uniquely or potently induced a number of tumor suppressor genes that might contribute to biological properties of PIAs that extend beyond inhibition of Akt. This expression profile could underlie their enhanced toxicity and could be utilized in pharmacodynamic studies of PIAs.

Materials and Methods

Cell Lines and Materials

NSCLC cell lines (H157, A549, H1703 and H1155) were obtained from NCI/Navy Medical Oncology (Bethesda, MD). They were maintained in RPMI medium 1640 with 10% (v/v) fetal bovine serum (FBS), and incubated at 37°C in a 5.0% CO_2 atmosphere. All lines were recently tested and authenticated by the Core Fragment Analysis Facility (Johns Hopkins University, Baltimore, MD) using a short tandem repeat (STR) profiling in accordance with AACR best practices. The synthesis of the PIAs has previously been described (11). LY294002 was purchased from Calbiochem (San Diego, CA). Antibodies to phospho-Akt (S473), Akt1, Akt2, Akt3, HSP70 and anti-mouse or anti-rabbit secondary antibodies were purchased from Cell Signaling Technologies (Beverly, MA). The DNA primase (p49) antibody was from Lab Vision Corporation (Fremont, CA). Antibodies to KLF6, MCM3, PCNA and IGFBP3 as well as anti-goat secondary antibody were purchased from Santa Cruz Biotechnology, Inc. (Santa Cruz, CA). RhoB antibody was purchased from Proteintech

Group, Inc. (Chicago, IL). Protease inhibitor cocktail tablets were obtained from Roche Diagnostics GmbH (Mannheim, Germany) and the Micro BCA Protein Assay Kit was from PIERCE (Rockford, IL). The pcDNA3-HA-RhoB was a kind gift from Dr. George Prendergast. The pCMV6-KLF6 and -CDKN1A were from OriGene (Rockville, MD). The pcDNA3-Myr-HA-Akt1 (24) was provided by Dr. William Sellers via Addgene (Cambridge, MA). RhoB, KLF6 and CDKN1A On-Target plus human siRNAs were from Dharmacon/Thermo (Lafayette, CO). Protran pure nitrocellulose membranes were purchased from Schleicher & Schuell (Dassel, Germany). All cell culture reagents were purchased from Life Technologies, Inc. (Rockville, MD).

Pharmacological Treatment and oligonucleotide microarray analysis

NSCLC cells were plated 2×10^5 cells per well in 6-well plates or 2×10^6 in T-75 flasks in RPMI medium 1640 containing 10% FBS and incubated for 24h. The medium was then changed to RPMI medium 1640 with 0.1% FBS and the cells were incubated overnight. The following morning, cells were treated with 10 μM PIA6 dissolved in DMSO for 0h, 2h, 6h or 12h, and an equal volume of DMSO was added to control samples. For the PIA comparison, 10 μM PIAs (5, 6, 7, 23, 24, 25) or 10 μM LY294002 (LY) were incubated with the cells for 6h. PIA7 (an inert analog consisting of only the lipid side chain) was used as a control. The structures of the PIAs and LY294002 are shown in Figure 1A. Cell viability was not affected in 0.1% FBS for the duration of these experiments. In cells cultured with 5% FBS, PIAs are highly bound to serum proteins and higher concentrations are needed to observe the same effects. Following incubation, the alterations in cellular morphology were photographed, and cells from 6-well plates were harvested for immunoblot analysis. Total RNA was extracted from cells treated in T-75 flasks using TRIzol reagent (Invitrogen) and chloroform and purified according to the RNeasy midiprep spin kit protocol (Qiagen). Oligonucleotide microarray was performed with dye-swap. Microarray chips were generated from the 34,580 longmer probe set Human Genome Oligo Set Version 3.0 (Qiagen). Protocols for cDNA labeling, hybridization, and scanning are available through the National Human Genome Research Institute microarray core. The raw data were deposited in a public functional genomics data repository Gene Expression Omnibus (GSE27911; ref. 25). Immunoblotting analysis was performed as described previously (26).

RT-PCR

Semi-quantitative RT-PCR was performed using the SuperScript™ One-Step RT-PCR System with Platinum® *Taq* DNA polymerase (Invitrogen). The following forward and reverse primers were used: (1) DUSP1, 5′-ctgccttgatcaacgtctca-3′ and 5′-acccttcctccagcattctt-3′; (2) KLF6, 5′-ggcaacagacctgcctagag-3′ and 5′-aggattcgctgctgacatct-3′; (3) CEND2, 5′-gctttggaggtcaacgagagg-3′ and 5′-gaagtagcgatcgtggaagc-3′; (4) BHLHB2, 5′-ccttgaagcatgtgaaagca-3′ and 5′-gcttggccagatactgaagc-3; (5) PREX1, 5′-ccctggtcagtgaagagagc-3′ and 5′-tcatctccagaccccatctc-3′; (6) TRIB1, 5′-tctggctttgaggcttgttt-3′ and 5′-cagcccagagtccttagtcg-3′; (7) KLF2, 5′-agagggtctccctcgatgac-3′ and 5′-tctcacaaggcatcacacaagc-3′; (8) RHOB, 5′-cgacgtcattctcatgtgct-3′ and 5′-cgaggtagtcgtaggcttgg-3′; (9) CDKN1A, 5′-atgaaattcacccccttttcc-3′ and 5′-ccctaggctgtgctcacttc-3′; (10) C21orf58, 5′-cctcttccatcacggaggta-3′ and 5′-ggcacacaggtgtccctagt; (11) IGFBP3, 5′-cagagactcgagcacagcac-3′ and 5′-gatgaccgggggtttaaaggt-3′; (12) PCNA, 5′-ggcgtgaacctcaccagtat-3′ and 5′-tctcggcatatacgtgcaaa-3′; (13) PRIM1, 5′-gccatacgcatcattgacag-3′ and 5′-ccacccttta caaggctcaa-3′; (14) MCM3, 5′-cgcaggaaaaacgagaagag-3′ and 5′-cagaccacacagctgaggaa-3′; (15) HSPA1B, 5′-ccgagaaggacgagtttgag-3′ and 5′-gcagcaaagtccttgagtcc-3′; (16) GAPDH, 5′-gagtcaacggatttggtcgt-3′ and 5′-ttgattttggagggatctcg-3′.

Bioinformatics Tools for Gene Clustering, Visualization and Ontology

The microarray outputs were clustered and visualized by Cluster 3.0 (27) and Java TreeView (28). Gene expression dynamics was analyzed by CAGED program (Cluster Analysis of Gene Expression Dynamics) (29). For gene ontology analysis, the High-Throughput GoMiner web interface (30) was used as described (31).

Cell Transfection and Infection

Transfection of plasmid or siRNA was performed with a Nucleofector device using program T-16 and transfection kit V (Lonza). Cells stably expressing Myr-Akt1 were created following plasmid transfection by G418 (800 μg/ml) selection for 2 weeks. Cell lines expressing Akt isoform specific shRNAs were created by lentiviral infection and shRNA vectors used were from Sigma-Aldrich unless otherwise noted: Akt1, NM_005163.1-628s1c1; Akt2, NM_001626.2-1509s1c1; Akt3, NM_005465.3-671s1c1; non-targeting, pLKO-scr (Addgene). Gene overexpression or knockdown was verified by immunoblotting.

MTS Assay and FACS Analysis

The MTS assay was performed with CellTiter 96 Aqueous One Solution Reagent (Promega) according to the manufacturer's instructions, and the cell viability was determined by measuring the absorbance at 490 nm using a BioTek ELx800 Microplate Reader. Apoptosis (sub-G1 DNA) was quantified by propidium iodide staining and analysis using a Becton Dickinson FACSort flow cytometer and CELLQuest software.

Results

Optimization of PIA Treatments and Microarray Analysis

Preliminary experiments were performed to optimize conditions for microarray analysis. Previously, we observed that PIAs cause profound morphologic changes in NSCLC cells, including rounding and detachment. To assess the time dependence of these changes, H157 cells were treated with PIA6 and observed over time (Figure 1B). At 2h, there was little morphologic change, but by 6h, the cells had become highly refractile and rounded. Between 6 and 12h, cellular detachment occurred. Similar time dependent changes were observed with other active PIAs, but not an inactive PIA (PIA7) or LY (data not shown). In addition, PIA exposure caused similar morphologic changes in other NSCLC cell lines, but with different kinetics. For example, these changes were delayed in A549 and H1703 cells, but accelerated in H1155 cells (data not shown). In H157 cells treated with PIA6, the surviving fractions measured by MTS assay at 2, 6 and 12h were 95%, 79% and 48%, respectively. These experiments suggest that at treatment times up to 6h, cellular detachment would not confound the measurement of gene expression changes induced by PIAs.

To assess Akt inhibition, immunoblotting was performed with parallel samples prepared from H157 cells (Figure 1C). PIA6 inhibited Akt phosphorylation at S473 at 2, 6 and 12h (left panels). Treatment with any of 5 active PIAs or LY also decreased S473 phosphorylation in H157 cells at 6h (right panels). PIA7, an analog that lacks the inositol ring, did not inhibit Akt phosphorylation. To assure that RNA quality and integrity were maintained with increasing times of exposure to PIAs, analysis using a Bioanalyzer Nanochip was performed. The 28S and 18S rRNA bands were sharp up to 12h and the 28S bands were more intense than 18S bands, indicating the RNA quality was adequate (Fig. 1D, left panels). RNA integrity was also preserved in samples treated with all PIAs or LY for 6h (Fig. 1D, right panels). Based on the assessment of cellular morphology, Akt inhibition and RNA quality, 6h was chosen as the time point at which to compare changes in gene expression with PIAs and LY.

Following microarray analysis, 911 genes were identified that exhibited differential expression by treatment with one or more of the 5 active PIAs in H157 cells (using a cutoff of a 2-fold change in expression). A hierarchical clustered heat map and cluster tree of these data is presented in Figure 1E. The expression of genes in response to LY is shown in the far right column. Clustering of expression signatures revealed that PIA23 and PIA25 showed the highest degree of similarity to each other. Although PIA5 showed similarity to PIA24, it altered fewer genes and many less potently than PIA24. PIA6 shared the most genes in common with the other 4 according to the clustering and was relatively close to the PIA23 and PIA25 subgroup.

To quantify genes that changed in common with PIAs and LY, Venn Mapper (32) was used to calculate the number of differentially expressed genes that overlapped between each PIA treatment and LY, as well as the corresponding Z-scores (Supplemental Table 1). Of genes that increased, PIA23 and PIA25 each shared 33 genes with LY, with the highest positive Z-scores of 5.8 and 7.2, respectively. However, PIA5, 6, and 24 had little overlap with LY, resulting in negative Z-scores. Of genes that decreased, PIA5, 6, 23, 24 and 25 had 13, 11, 43, 25 and 35 genes in common with LY, respectively, all with positive Z-scores (1.0, 4.5, 9.3, 3.3 and 8.2, respectively). Given that the cutoff Z-score for statistical significance (a p-value of <0.05) was 1.96 or greater (http://www.gatcplatform.nl/vennmapper/index.php), these data indicate that PIA6, 23, 24 and 25 shared genes that decreased in common with LY in a statistically significant manner, but only PIA23 and 25 shared genes that increased in common with LY in a statistically significant manner (99.9% confidence level). Interestingly, the Z-scores between any two PIAs were positive for increased or decreased comparisons but negative at increased-decreased or decreased-increased comparisons, suggesting these compounds affected gene expression in a similar direction but to different extents. The complete list of differentially expressed genes and enlarged heat map are shown in Supplemental Table 2 and Supplemental Figure 1.

Early Changes in Gene Expression Caused in Common by PIAs

From the clustered heat map, 83 transcripts were identified that were similarly regulated (either positively or negatively) by all 5 active PIAs. These were partitioned into 4 gene categories (C1-4) using k-Means clustering (Fig. 2A). C1 and C2 were likely due to Akt pathway inhibition, since C1 includes genes that were induced by PIAs and LY, and C2 includes genes that were repressed by both PIAs and LY. C3 and C4 include PIA specific genes that are either repressed or induced by PIAs, respectively.

To identify the earliest changes in gene expression that occurred following PIA treatment, a time course experiment was performed. RNA was isolated after 0, 2, 6 or 12h exposure to PIA6. Sixty genes were extracted from 83 transcripts similarly regulated by PIAs at the 4 time points, and their expression levels with PIA6 exposure are depicted in Fig. 2B. Because temporal patters of gene expression can be useful to identify common regulatory mechanisms, a temporal cluster analysis was performed using the CAGED program (Cluster Analysis of Gene Expression Dynamics). This program identified 15 clusters that exhibited distinct dynamic patterns over time, with 4 genes for each cluster (Fig. 2C, and Supplemental Figure 2). Because we wanted to identify the early and constitutively up-regulated or down-regulated genes that changed with time, clusters 2, 3, 6, 11, 14 and 15 were chosen for further analysis. The 24 genes from these 6 clusters were further partitioned based on data from the PIA and LY comparisons, as well as the time course experiments (10 different conditions using CAGED), which generated 3 groups that exhibited similar patterns (Fig. 2D). The genes in groups I and II were upregulated by PIAs. Group I is characterized by genes not induced by LY. Group II is characterized by genes more strongly induced by PIA treatment, but commonly induced by LY. In contrast, group III genes were downregulated by PIAs and in most cases, LY. The degree of downregulation caused by

PIAs was similar to that of LY. The identity of genes comprising these groups, along with attributions of their function, process and subcellular location, is listed in Fig. 2E.

Validation of Microarray Data

Changes in gene expression depicted in Groups I-III were validated using semi-quantitative RT-PCR (Fig. 3A). Time dependence (left panels) and specificity for individual PIAs vs. LY (right panels) were assessed. From group I, *DUSP1*, *KLF6*, *CENTD2*, *BHLHB2* and *PREX1* were selected for validation. *KLF6* and *DUSP1* were strongly induced by PIA6 from 2h to 12h, *CENTD2* and *BHLHB2* were slightly induced at 2h and strongly induced from 6h to 12h, and *PREX1* was induced beginning at 6h. The mRNA levels of *DUSP1*, *CENTD2*, *BHLHB2* and *PREX1* were increased in the DMSO-treated sample at 12h, indicating that these genes may be sensitive to culture conditions such as nutrient consumption and/or increases in cell density. *DUSP1*, *KLF6*, *CENTD2*, *BHLHB2* and *PREX1* were all induced by the 5 active PIAs, and not by LY or PIA7. These data confirm that these genes are rapidly induced by PIAs and are selective for active PIAs.

The 4 genes chosen from group II, *TRIB1*, *KLF2*, *RHOB* and *CDKN1A*, were induced by PIA6 from 2h to 12h. In particular, *RHOB* and *KLF2* were strongly induced at early time points. The basal level of *KLF2* expression was hardly detectable, and its induction appeared transient with peak expression at 2h. Induction of *TRIB1* and *KLF2* was not selective for PIAs, because LY had similar effects (Figure 3A, middle-right panel). *RHOB* and *CDKN1A* were also induced by the 5 active PIAs, but were less potently by LY. Although individual variation was observed, expression of these genes from group II was similarly regulated by PIAs and LY, suggesting that these changes were likely due to inhibition of the PI3K/Akt pathway.

Six genes were chosen from group III for validation. Expression of *IGFBP3*, *PCNA* and *PRIM1* decreased from 2h to 12h. Decreased expression of *C21orf58*, *MCM3* and *HSPA1B* was evident from 6h to 12h. When assessed for specificity between PIAs and LY, group III genes were repressed by both PIAs and LY, except for *C21orf58*, which was not inhibited by LY. Collectively, the expression of these genes as assessed by RT-PCR is in agreement with the microarray data.

To confirm that changes in mRNA expression would lead to protein level alterations, immunoblotting was performed (Fig. 3B). Due to limited availability of reliable antibodies, only a subset of the genes could be assessed. From group I, KLF6 protein expression increased after PIA treatment in 4 NSCLC cell lines. From group II, PIA treatment increased CDKN1A expression and markedly induced RhoB expression. When genes from group III were analyzed, the protein levels of PIA-repressed genes such as IGFBP3, PCNA, MCM3 and HSPA1B did not appreciably decrease at 6h. This could be related to slow protein turnover. To test this, we performed a longer time course and found these proteins were decreased at 12h and 24h (Fig. 3C). These immunoblotting experiments validate protein expression as a readout for genes that are regulated by PIAs.

Identification of biologically-relevant gene categories altered by PIAs

To explore the biological significance of the microarray data, gene ontology analysis was performed by uploading the total gene list represented on the chip, along with the induced or repressed genes, into the High-Throughput GoMiner web interface. A summary of this analysis from the 6h PIA comparison experiment is presented in Table 1. The "total genes" column indicates how many genes on the chip were assigned to the respective categories. The "changed genes" column indicates how many of the genes that changed significantly (>2 fold) during treatment were assigned to the targeted GO categories. The enrichment, *p*

value and false discovery rate (FDR) of the GO categories were calculated and listed with an FDR cutoff of <0.05. Some general categories such as regulation of cellular, physiological or biological processes had the lowest *p*-values, yet these communicate little meaning. The categories with the next most significant *p*-values were more relevant, namely apoptosis and cell death, followed by response to wounding, cell cycle, and angiogenesis. Apoptosis is a known cellular outcome of PIA treatment (12). The "under-expressed" GO category result indicates genes associated with DNA-dependent DNA replication were inhibited by PIAs. The individual genes assigned to these GO categories are listed in Supplementary Table 3.

Time dependent changes in gene ontology were also assessed (Table 2). The categories of genes induced earliest were death-related. This process continued and was further defined as apoptosis from 6h to 12h. By 12h, several categories were added, including protein and macromolecule biosynthesis, wound healing, and angiogenesis. The first categories of repressed genes included DNA-dependent DNA replication and cell cycle regulation, which were only evident beginning at 6h. By 12h, several other categories were added, similar to the observations with induced genes. Collectively, the gene ontology analysis suggests that although PIAs induce changes in expression of a fairly small number of genes, these changes become manifest by altering many cellular processes in ways that would likely be detrimental to the growth and survival of cancer cells.

Akt dependence and responses to PIAs

Although a COMPARE analysis indicated the cytotoxicity of PIAs correlated with active Akt levels (13), a functional analysis between PIA cytotoxicity and Akt activation in an isogenic system has not been done. To address this, we created an H157 cell line stably transfected with constitutively active MyrAkt1. Although MyrAkt1-expressing cells showed lower basal levels of apoptosis as indicated by cleaved PARP and sub-G1 DNA content, apoptosis was further induced with PIA23 treatment (Fig. 4A). Similar results were observed when other apoptotic assays such as Annexin-V/PI co-staining were employed (data not shown). These findings were confirmed in an A549 isogenic system, in which the 3 Akt isoforms were individually stably knocked down by lentiviral infection with shRNAs. Immunoblotting confirmed Akt isoform specific knockdown, and also demonstrated that Akt1 was the major isoform in A549 cells, because only Akt1 knockdown decreased levels of total and phospho-Akt. Accordingly, only Akt1 knockdown resulted in significantly less apoptotic cell death with PIA treatment (Fig. 4B). These studies demonstrated levels of active Akt, specifically Akt1, correlated with PIA cytotoxicity.

To address the Akt-dependence of PIA-induced genes, we used genetic or pharmacologic approaches to modulate Akt, and measured levels of RhoB, KLF6, and p21 after PIA treatment. In H157 cells transfected with MyrAkt1 or vector, induction of RhoB, KLF6 or p21 by PIA23 was observed (Fig. 4C). Although the induction of KLF6 and p21 by PIA23 in MyrAkt1 transfected cells appears slightly diminished compared to vector transfected cells, this is likely an artifact related to lower expression of p42/44 MAPK under these experimental conditions, which was observed in replicate experiments. When Akt1 was knocked down in A549 cells, the induction of RhoB, KLF6 and p21 by PIA23 was not affected (Fig. 4D). To confirm these results, we pretreated H157 cells with LY for 30 min followed by 6h treatment with PIA23. LY alone slightly induced RhoB, KLF6 and p21 protein levels, but the combination of LY with PIA23 enhanced the expression of the PIA-induced genes over either compound alone (Fig. 4E). These results indicate that induction of these tumor suppressors is only minimally dependent upon the Akt pathway.

An important question is whether any of PIA-induced genes identified contribute to the cytotoxicity of the compounds. To examine this, H157 cells were transiently transfected with *RHOB*, *KLF6* or *CDKN1A* siRNAs and treated with PIA 48h later. Cell lysates were

harvested after 6h to assess knockdown, and sub-G1 DNA analysis was performed after 12h PIA treatment. The results show that although the siRNAs did not entirely block the induction of their target genes, these greatly rescued H157 cells from apoptosis caused by PIA (Fig. 4F). In contrast, overexpression of these genes either individually or in combination significantly decreased the viability of H157 cells (Fig. 4G). Similar results were observed in other NSCLC cell lines such as H1155 and H2882, and in other cancer cell lines with high levels of endogenous Akt activation (data not shown). These data confirm RhoB, KLF6 and p21 induction contribute to the cytotoxicity of PIAs.

Discussion

Using microarray analysis, we identified gene expression profiles that contribute to the biologic effects of PIAs. Validation of individual gene changes using RT-PCR and immunoblotting showed that microarray results could be validated at both the mRNA and protein levels, albeit protein level decreases were delayed as compared to mRNA decreases for the PIA-suppressed genes. The fact that induction of genes by PIAs could be measured by PCR or immunoblotting suggests that these genes could serve as biomarkers for PIA administration.

To place these individual changes in gene expression in a biologic framework, gene ontology analysis was performed and revealed that many cellular processes are altered due to PIA-induced changes in gene expression in a time-dependent manner. Early induction of apoptosis or cell death and repression of DNA replication and cell cycle were observed after PIA administration, which is consistent with development of PIAs as anti-cancer agents. Of the early-induced genes, KLF6, RHOB/RhoB and CDKN1A/p21 were of particular interest because they are known tumor suppressors and their expression reduced overall cell viability and contributed to PIA-induced cytotoxicity.

RhoB is a small GTPase tumor suppressor that regulates actin organization and vesicle transport. It is required for signalling apoptosis in transformed cells that are exposed to chemotherapeutic agents, has a negative modifier function in carcinogenesis (33), and its expression is repressed during NSCLC progression (34–36). Although RhoB has a reciprocal relationship with levels of Akt activation in cells (37, 38), our studies showed that inhibition of Akt through genetic or pharmacologic means did not significantly affect induction of RhoB by PIAs. This suggests a novel mechanism for RhoB induction by PIAs.

CDKN1A/p21 inhibits cell cycle by binding to cyclin/CDK complexes and PCNA in nucleus, which can be prevented by Akt via phosphorylation (39). Because induction of p21 was observed in cell lines that have either WT (A549) or mutant p53 (H157, H1703 and H1155), induction of p21 by PIAs is p53-independent. This observation is consistent with p53-independent induction of p21 by perifosine, an alkylphospholipid whose activity correlated highly with PIAs (13, 40). Interestingly, the induction of RhoB and p21 by PIAs might be related, because PPARγ-mediated induction of p21 in anaplastic thyroid carcinoma is dependent upon up-regulation of RhoB (41).

KLF6 is a member of the Krüppel-like factor family of C2H2-type zinc finger-containing transcription factors implicated in cellular differentiation and tissue development (42). The KLF6 gene encodes a family of proteins generated through alternative splicing, which results in at least four isoforms. Full length KLF6 is a tumor suppressor that is frequently inactivated by loss of heterozygosity (LOH), somatic mutation, and/or decreased expression in human cancer. Its tumor suppressor roles are not completely known, but a number of highly relevant activities have been described such as transactivation of p21 in a p53-

independent manner (43, 44), reduction of cyclin D1/cdk4 complexes via interaction with cyclin D1 (45), and induction of apoptosis through up-regulation of ATF3 (46).

Genetic manipulation demonstrated that active Akt1 is a predictor of PIA efficacy in NSCLC cells since expression of constitutively active Akt increased cytotoxicity and knockdown of Akt1 protected against PIA-induced cytotoxicity. PIA treatment induced expression of KLF6, RHOB/RhoB and CDKN1A/p21 in a mostly Akt-independent manner. Nonetheless, these tumor suppressors inhibited cellular viability when overexpressed, and contributed to the cytotoxicity of PIAs. These studies suggest that the broad activity of PIAs against cancer cells is based upon multiple independent mechanisms that include inhibition of Akt (12) and activation of p38α (47) and AMPKα (26), as well as induction of tumor suppressor genes such as KLF6, RhoB and p21. As a result, the development of biomarkers for PIAs will be complex and will need to account for PIA-induced changes in enzymatic activity as well as gene transcription.

Supplementary Material

Refer to Web version on PubMed Central for supplementary material.

Acknowledgments

Abbreviations

PI3K	phosphatidylinositol 3′ kinase
NSCLC	non-small cell lung cancer
PIA	phosphatidylinositol ether lipid analogue
LY	LY294002
MAPK	mitogen-activated protein kinase

References

1. LoPiccolo J, Granville CA, Gills JJ, Dennis PA. Targeting Akt in cancer therapy. Anticancer Drugs. 2007; 18:861–74. [PubMed: 17667591]

2. Brognard J, Clark AS, Ni Y, Dennis PA. Akt/protein kinase B is constitutively active in non-small cell lung cancer cells and promotes cellular survival and resistance to chemotherapy and radiation. Cancer Res. 2001; 61:3986–97. [PubMed: 11358816]

3. Clark AS, West K, Streicher S, Dennis PA. Constitutive and inducible Akt activity promotes resistance to chemotherapy, trastuzumab, or tamoxifen in breast cancer cells. Mol Cancer Ther. 2002; 1:707–17. [PubMed: 12479367]

4. Granville CA, Memmott RM, Gills JJ, Dennis PA. Handicapping the race to develop inhibitors of the phosphoinositide 3-kinase/Akt/mammalian target of rapamycin pathway. Clin Cancer Res. 2006; 12:679–89. [PubMed: 16467077]

5. LoPiccolo J, Blumenthal GM, Bernstein WB, Dennis PA. Targeting the PI3K/Akt/mTOR pathway: effective combinations and clinical considerations. Drug Resist Updat. 2008; 11:32–50. [PubMed: 18166498]

6. West KA, Brognard J, Clark AS, Linnoila IR, Yang X, Swain SM, et al. Rapid Akt activation by nicotine and a tobacco carcinogen modulates the phenotype of normal human airway epithelial cells. J Clin Invest. 2003; 111:81–90. [PubMed: 12511591]

7. Tsurutani J, Castillo SS, Brognard J, Granville CA, Zhang C, Gills JJ, et al. Tobacco components stimulate Akt-dependent proliferation and NFkappaB-dependent survival in lung cancer cells. Carcinogenesis. 2005; 26:1182–95. [PubMed: 15790591]

8. West KA, Linnoila IR, Brognard J, Belinsky S, Harris C, Dennis PA. Tobacco carcinogen-induced cellular transformation increases Akt activation in vitro and in vivo. Chest. 2004; 125 (Suppl 5): 101–2.

9. Granville CA, Warfel N, Tsurutani J, Hollander MC, Robertson M, Fox SD, et al. Identification of a highly effective rapamycin schedule that markedly reduces the size, multiplicity, and phenotypic progression of tobacco carcinogen-induced murine lung tumors. Clin Cancer Res. 2007; 13:2281–9. [PubMed: 17404113]

10. Tsurutani J, Fukuoka J, Tsurutani H, Shih JH, Hewitt SM, Travis WD, et al. Evaluation of two phosphorylation sites improves the prognostic significance of Akt activation in non-small-cell lung cancer tumors. J Clin Oncol. 2006; 24:306–14. [PubMed: 16330671]

11. Kozikowski AP, Sun H, Brognard J, Dennis PA. Novel PI analogues selectively block activation of the pro-survival serine/threonine kinase Akt. J Am Chem Soc. 2003; 125:1144–5. [PubMed: 12553797]

12. Castillo SS, Brognard J, Petukhov PA, Zhang C, Tsurutani J, Granville CA, et al. Preferential inhibition of Akt and killing of Akt-dependent cancer cells by rationally designed phosphatidylinositol ether lipid analogues. Cancer Res. 2004; 64:2782–92. [PubMed: 15087394]

13. Gills JJ, Holbeck S, Hollingshead M, Hewitt SM, Kozikowski AP, Dennis PA. Spectrum of activity and molecular correlates of response to phosphatidylinositol ether lipid analogues, novel lipid-based inhibitors of Akt. Mol Cancer Ther. 2006; 5:713–22. [PubMed: 16546986]

14. Cho RJ, Huang M, Campbell MJ, Dong H, Steinmetz L, Sapinoso L, et al. Transcriptional regulation and function during the human cell cycle. Nat Genet. 2001; 27:48–54. [PubMed: 11137997]

15. Rhodes DR, Yu J, Shanker K, Deshpande N, Varambally R, Ghosh D, et al. Large-scale meta-analysis of cancer microarray data identifies common transcriptional profiles of neoplastic transformation and progression. Proc Natl Acad Sci U S A. 2004; 101:9309–14. [PubMed: 15184677]

16. Hardy K, Mansfield L, Mackay A, Benvenuti S, Ismail S, Arora P, et al. Transcriptional networks and cellular senescence in human mammary fibroblasts. Mol Biol Cell. 2005; 16:943–53. [PubMed: 15574883]

17. Ramaswamy S, Ross KN, Lander ES, Golub TR. A molecular signature of metastasis in primary solid tumors. Nat Genet. 2003; 33:49–54. [PubMed: 12469122]

18. LaGamba D, Nawshad A, Hay ED. Microarray analysis of gene expression during epithelial-mesenchymal transformation. Dev Dyn. 2005; 234:132–42. [PubMed: 16010672]

19. Bild AH, Yao G, Chang JT, Wang Q, Potti A, Chasse D, et al. Oncogenic pathway signatures in human cancers as a guide to targeted therapies. Nature. 2006; 439:353–7. [PubMed: 16273092]

20. Strand KJ, Khalak H, Strovel JW, Ebner R, Augustus M. Expression biomarkers for clinical efficacy and outcome prediction in cancer. Pharmacogenomics. 2006; 7:105–15. [PubMed: 16354128]

21. van't Veer LJ, Dai H, van de Vijver MJ, He YD, Hart AA, Mao M, et al. Gene expression profiling predicts clinical outcome of breast cancer. Nature. 2002; 415:530–6. [PubMed: 11823860]

22. Butcher RA, Schreiber SL. Using genome-wide transcriptional profiling to elucidate small-molecule mechanism. Curr Opin Chem Biol. 2005; 9:25–30. [PubMed: 15701449]

23. Marton MJ, DeRisi JL, Bennett HA, Iyer VR, Meyer MR, Roberts CJ, et al. Drug target validation and identification of secondary drug target effects using DNA microarrays. Nat Med. 1998; 4:1293–301. [PubMed: 9809554]

24. Ramaswamy S, Nakamura N, Vazquez F, Batt DB, Perera S, Roberts TM, et al. Regulation of G1 progression by the PTEN tumor suppressor protein is linked to inhibition of the

phosphatidylinositol 3-kinase/Akt pathway. Proc Natl Acad Sci U S A. 1999; 96:2110–5. [PubMed: 10051603]

25. Gene Expression Omnibus. The National Center for Biotechnology Information (NCBI). NIH; Available from: http://www.ncbi.nlm.nih.gov/geo

26. Memmott RM, Gills JJ, Hollingshead M, Powers MC, Chen Z, Kemp B, et al. Phosphatidylinositol ether lipid analogues induce AMP-activated protein kinase-dependent death in LKB1-mutant non small cell lung cancer cells. Cancer Res. 2008; 68:580–8. [PubMed: 18199555]

27. Available from: http://bonsai.ims.u-tokyo.ac.jp/~mdehoon/software/cluster/software.htm#ctv.

28. Available from: http://sourceforge.net/projects/jtreeview.

29. Available from: http://www.genomethods.org/caged.

30. Available: http://discover.nci.nih.gov/gominer/htgm.jsp.

31. Zeeberg BR, Qin H, Narasimhan S, Sunshine M, Cao H, Kane DW, et al. High-Throughput GoMiner, an 'industrial-strength' integrative gene ontology tool for interpretation of multiple-microarray experiments, with application to studies of Common Variable Immune Deficiency (CVID). BMC Bioinformatics. 2005; 6:168. [PubMed: 15998470]

32. Smid M, Dorssers LC, Jenster G. Venn Mapping: clustering of heterologous microarray data based on the number of co-occurring differentially expressed genes. Bioinformatics. 2003; 19:2065–71. [PubMed: 14594711]

33. Prendergast GC. Actin' up: RhoB in cancer and apoptosis. Nat Rev Cancer. 2001; 1:162–8. [PubMed: 11905808]

34. Wang S, Yan-Neale Y, Fischer D, Zeremski M, Cai R, Zhu J, et al. Histone deacetylase 1 represses the small GTPase RhoB expression in human nonsmall lung carcinoma cell line. Oncogene. 2003; 22:6204–13. [PubMed: 13679859]

35. Sato N, Fukui T, Taniguchi T, Yokoyama T, Kondo M, Nagasaka T, et al. RhoB is frequently downregulated in non-small-cell lung cancer and resides in the 2p24 homozygous deletion region of a lung cancer cell line. Int J Cancer. 2007; 120:543–51. [PubMed: 17096327]

36. Mazieres J, Tovar D, He B, Nieto-Acosta J, Marty-Detraves C, Clanet C, et al. Epigenetic regulation of RhoB loss of expression in lung cancer. BMC Cancer. 2007; 7:220. [PubMed: 18047684]

37. Jiang K, Delarue FL, Sebti SM. EGFR, ErbB2 and Ras but not Src suppress RhoB expression while ectopic expression of RhoB antagonizes oncogene-mediated transformation. Oncogene. 2004; 23:1136–45. [PubMed: 14647415]

38. Jiang K, Sun J, Cheng J, Djeu JY, Wei S, Sebti S. Akt mediates Ras downregulation of RhoB, a suppressor of transformation, invasion, and metastasis. Mol Cell Biol. 2004; 24:5565–76. [PubMed: 15169915]

39. Zhou BP, Liao Y, Xia W, Spohn B, Lee MH, Hung MC. Cytoplasmic localization of p21Cip1/WAF1 by Akt-induced phosphorylation in HER-2/neu-overexpressing cells. Nat Cell Biol. 2001; 3:245–52. [PubMed: 11231573]

40. Patel V, Lahusen T, Sy T, Sausville EA, Gutkind JS, Senderowicz AM. Perifosine, a novel alkylphospholipid, induces p21(WAF1) expression in squamous carcinoma cells through a p53-independent pathway, leading to loss in cyclin-dependent kinase activity and cell cycle arrest. Cancer Res. 2002; 62:1401–9. [PubMed: 11888912]

41. Marlow LA, Reynolds LA, Cleland AS, Cooper SJ, Gumz ML, Kurakata S, et al. Reactivation of suppressed RhoB is a critical step for the inhibition of anaplastic thyroid cancer growth. Cancer Res. 2009; 69:1536–44. [PubMed: 19208833]

42. Atkins GB, Jain MK. Role of Kruppel-like transcription factors in endothelial biology. Circ Res. 2007; 100:1686–95. [PubMed: 17585076]

43. Li D, Yea S, Dolios G, Martignetti JA, Narla G, Wang R, et al. Regulation of Kruppel-like factor 6 tumor suppressor activity by acetylation. Cancer Res. 2005; 65:9216–25. [PubMed: 16230382]

44. Narla G, Heath KE, Reeves HL, Li D, Giono LE, Kimmelman AC, et al. KLF6, a candidate tumor suppressor gene mutated in prostate cancer. Science. 2001; 294:2563–6. [PubMed: 11752579]

45. Benzeno S, Narla G, Allina J, Cheng GZ, Reeves HL, Banck MS, et al. Cyclin-dependent kinase inhibition by the KLF6 tumor suppressor protein through interaction with cyclin D1. Cancer Res. 2004; 64:3885–91. [PubMed: 15172998]

46. Huang X, Li X, Guo B. KLF6 induces apoptosis in prostate cancer cells through up-regulation of ATF3. J Biol Chem. 2008; 283:29795–801. [PubMed: 18755691]

47. Gills JJ, Castillo SS, Zhang C, Petukhov PA, Memmott RM, Hollingshead M, et al. Phosphatidylinositol ether lipid analogues that inhibit AKT also independently activate the stress kinase, p38alpha, through MKK3/6-independent and -dependent mechanisms. J Biol Chem. 2007; 282:27020–9. [PubMed: 17631503]
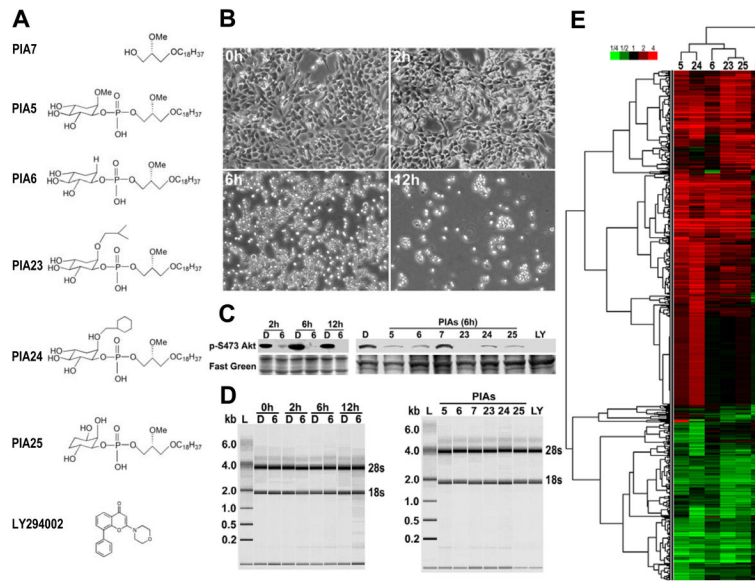
Figure 1.
Optimization of PIA treatment and oligonucleotide microarray analysis. **A)** The chemical structures of the inactive PIA7, 5 active PIAs and PI3K inhibitor LY294002. **B)** Cellular morphological alterations induced by PIA treatment. H157 cells were incubated with 10 μM PIA6 dissolved in DMSO in RPMI1640 + 0.1% FBS media for the indicated times. **C)** Evaluation of Akt inhibition in samples collected for microarray analysis. Parallel H157 cell samples were collected for analysis of p-S473 Akt by immunoblot, alongside microarray samples for RNA extraction, in time course and PIA comparison experiments as described in Materials and Methods. D = DMSO, 5, 6, 7, 23, 24, 25 = 10 μM PIA-treated samples, LY = 10 μM LY294002-treated sample. **D)** Assessment of RNA quality and integrity in microarray samples using the Bioanalyzer Nanochip. Prominent bands indicate positions of 28s and 18s rRNA. **E)** Clustered heat map showing PIA-altered genes. Red color = induction, green color = suppression, black color = no change in expression. Complete linkage hierarchical clustering of PIA-regulated gene expression changes in H157 cells was performed with uncentered correlation as described in Materials and Methods.
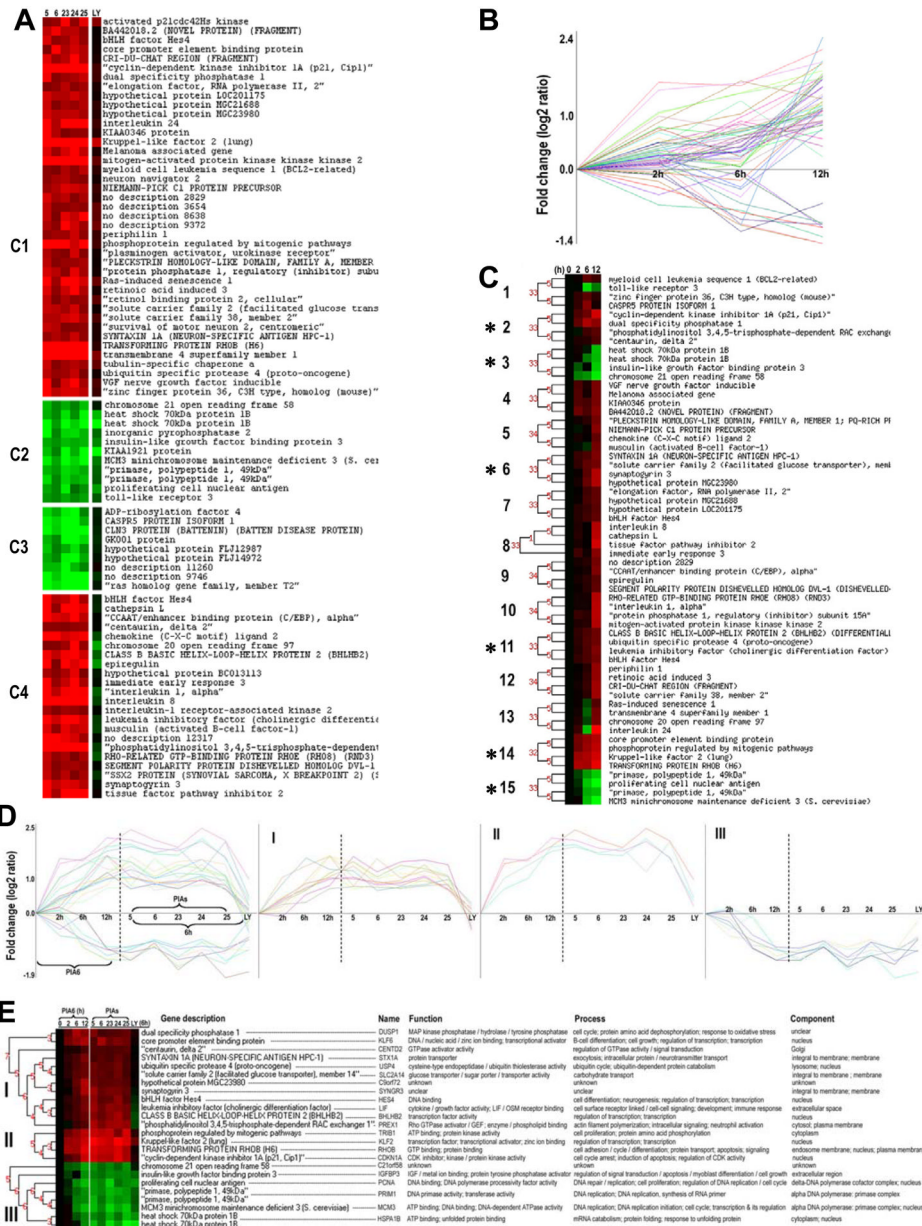
Figure 2.

Identification of genes that changed early and in common with PIA or LY treatment. **A)** Filtered set of common PIA-regulated genes grouped using k-Means clustering. C1 = genes that were induced by all 5 active PIAs and the PI3K inhibitor LY, C2 = genes suppressed by active PIAs and LY, C3 = genes suppressed by PIAs but not LY, C4 = genes that were induced by PIAs only, not LY. **B)** Temporal dynamics of common PIA-regulated genes. Expression levels of common PIA-regulated genes from figure 2A were extracted from PIA6 time course experiment and are depicted at the different time points. **C)** 15 temporal clusters of genes from figure 2B whose expression changed in a similar manner generated by CAGED program. The asterisks mark clusters (2, 3, 6, 11, 14 and 15) that were chosen for further analysis. **D)** Depiction of genes that were commonly regulated by PIAs and their temporal dynamics. Group I = genes induced early by PIAs but not LY, group II = genes

induced early and in common with LY, group III = genes suppressed early by PIAs and in common with LY. **E)** Identity, function and cellular location of Group I-III genes.
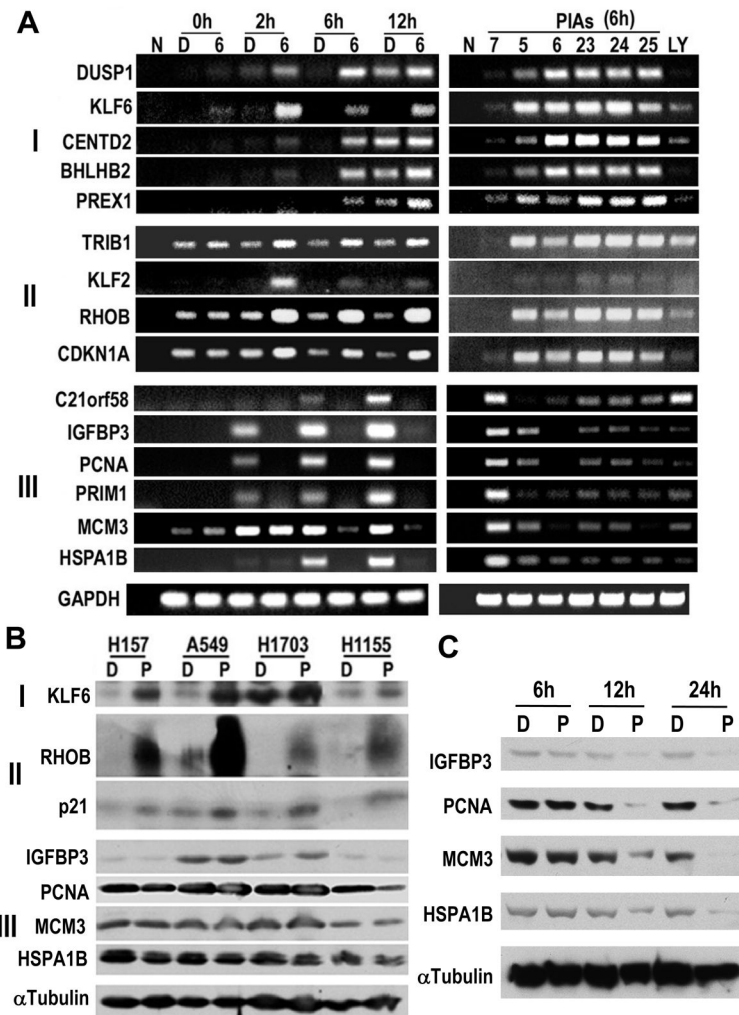
Figure 3.
Validation of microarray data by RT-PCR and immunoblotting. **A)** Validation of oligonucleotide microarray data by semi-quantitative RT-PCR. Expression of genes from groups I, II and III were evaluated in time course (left panels) and PIA comparison experiments (right panels). N = RNA omitted negative control. **B)** Immunoblotting analysis of KLF6, RhoB and p21 protein induction in vitro by PIA23 (6h) in 4 NSCLC cell lines. **C)** Protein expression of PIA-repressed transcripts in H157 cells decreases at later time points. D = DMSO, P = PIA23 (10 μM).
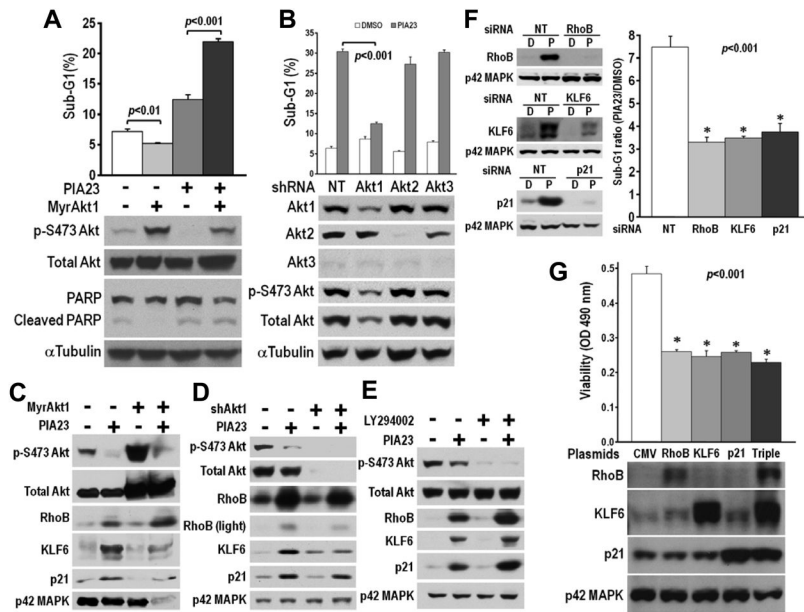
Figure 4.
Relevance of active Akt and induced genes to PIA-induced cytotoxicity. **A)** FACS analysis of sub-G1 DNA content and immunoblotting analysis of active Akt and cleaved PARP in MyrAkt1-expressing H157 cells treated with PIA23 (18h). **B)** Validation of Akt isoform specific knockdown by shAkt1, 2 or 3 in A549 cells and effect of individual stable knockdown on expression level of total and active Akt, as well as PIA23-induced apoptosis (24h). **C)** Expression of RhoB, KLF6 and p21 in MyrAkt1 or vector-expressing H157 cells treated with PIA23 (18h). **D)** Expression of RhoB, KLF6 and p21 in shAkt1 or non-targeting vector transfected A549 cells treated with PIA23 (24h). **E)** Expression of RhoB, KLF6 and p21 in H157 cells pretreated with LY294002 (0.5h), followed by treatment with PIA23 (6h). **F)** Effect of transient RhoB, KLF6, p21 or non-targeting (NT) siRNA transfection (48h) on protein induction by PIA23 (6h) and PIA-induced sub-G1 content in H157 cells (12h). **G)** Effect of overexpression of RhoB, KLF6 and p21 or the combination of all 3 genes on viability in H157 cells (48h). PIA23 and LY294002 = 10 μM. Data are means ± s.d. of triplicates and representative of 3 independent experiments.

Table 1

GeneOntology categories targeted by PIAs at 6h in H157 cells

OVEREXPRESSION					
GO CATEGORY	**TOTAL GENES**	**CHANGED GENES**	**ENRICHMENT**	**LOG10(p)**	**FDR**
GO:0050789_regulation_of_biological_process	2170	24	2.1105	−4.5343	0.0000
GO:0050791_regulation_of_physiological_process	1998	22	2.1012	−4.0073	0.0000
GO:0051244_regulation_of_cellular_physiological_process	1873	21	2.1395	−3.8992	0.0033
GO:0050794_regulation_of_cellular_process	1963	21	2.0414	−3.5890	0.0050
GO:0006915_apoptosis	356	8	4.2882	−3.3683	0.0080
GO:0012501_programmed_cell_death	358	8	4.2642	−3.3519	0.0067
GO:0008219_cell_death	377	8	4.0493	−3.2021	0.0086
GO:0016265_death	379	8	4.0280	−3.1868	0.0075
GO:0009611_response_to_wounding	324	7	4.1228	−2.8881	0.0300
GO:0048519_negative_regulation_of_biological_process	464	8	3.2901	−2.6194	0.0256
GO:0051243_negative_regulation_of_cellular_physiological_process	396	7	3.3732	−2.3934	0.0310
GO:0007050_cell_cycle_arrest	42	3	13.6304	−2.8766	0.0270
GO:0000074_regulation_of_cell_cycle	327	7	4.0849	−2.8648	0.0245
GO:0007049_cell_cycle	504	8	3.0290	−2.3968	0.0326
GO:0042330_taxis	109	4	7.0028	−2.6160	0.0228
GO:0006935_chemotaxis	109	4	7.0028	−2.6160	0.0228
GO:0048514_blood_vessel_morphogenesis	46	3	12.4451	−2.7616	0.0233
GO:0001525_angiogenesis	46	3	12.4451	−2.7616	0.0233
GO:0001568_blood_vessel_development	46	3	12.4451	−2.7616	0.0233
GO:0001944_vasculature_development	46	3	12.4451	−2.7616	0.0233
UNDEREXPRESSION					
GO:0006261_DNA-dependent_DNA_replication	58	3	26.3207	−3.7506	0.0400

Table 2

Time dependent changes in gene ontology caused by PIA6 treatment in H157 cells

GO CATEGORY	Changed/Total genes (FDR)		
OVEREXPRESSION	2h	6h	12h
GO:0001944_vasculature_development			10/46 (0.0227)
GO:0001568_blood_vessel_development			10/46 (0.0227)
GO:0048514_blood_vessel_morphogenesis			10/46 (0.0227)
GO:0001525_angiogenesis			10/46 (0.0227)
GO:0050878_regulation_of_body_fluids			16/98 (0.0238)
GO:0007599_hemostasis			15/87 (0.0209)
GO:0042060_wound_healing			15/87 (0.0209)
GO:0009611_response_to_wounding			41/324 (0.0200)
GO:0050817_coagulation			15/81 (0.0150)
GO:0007596_blood_coagulation			15/81 (0.0150)
GO:0006412_protein_biosynthesis			47/371 (0.0200)
GO:0009059_macromolecule_biosynthesis			49/409 (0.0133)
GO:0006915_apoptosis		8/356 (0.030)	43/356 (0.0129)
GO:0012501_programmed_cell_death	4/358 (0.05)	8/358 (0.015)	43/358 (0.0111)
GO:0008219_cell_death	4/377 (0.04)	8/377 (0.020)	45/377 (0.0200)
GO:0016265_death	4/379 (0.03)	8/379 (0.015)	45/379 (0.0125)
UNDEREXPRESSION			
GO:0006261_DNA-dependent_DNA_replication		3/58 (0.0100)	8/58 (0.0000)
GO:0006260_DNA_replication		3/113 (0.0118)	14/113 (0.0000)
GO:0006259_DNA_metabolism		5/365 (0.0075)	23/365 (0.0000)
GO:0006270_DNA_replication_initiation			5/14 (0.0000)
GO:0006310_DNA_recombination			5/48 (0.0076)
GO:0006139_nucleobase__nucleoside__nucleotide_and_nucleic_acid_metabolism			49/1892 (0.0000)
GO:0043283_biopolymer_metabolism			29/998 (0.0042)
GO:0006281_DNA_repair			13/142 (0.0000)
GO:0006974_response_to_DNA_damage_stimulus			14/157 (0.0000)
GO:0009719_response_to_endogenous_stimulus			14/166 (0.0000)
GO:0006950_response_to_stress			24/755 (0.0045)
GO:0007049_cell_cycle		6/504 (0.0050)	25/504 (0.0000)
GO:0000074_regulation_of_cell_cycle		5/327 (0.0100)	14/327 (0.0031)
GO:0051244_regulation_of_cellular_physiological_process		10/1873 (0.0071)	42/1873 (0.0368)
GO:0000279_M_phase			9/149 (0.0038)
GO:0051301_cell_division			8/119 (0.0033)
GO:0000910_cytokinesis			8/119 (0.0033)
GO:0000278_mitotic_cell_cycle			10/177 (0.0040)
GO:0000086_G2_M_transition_of_mitotic_cell_cycle			4/37 (0.0245)

GO CATEGORY	Changed/Total genes (FDR)		
OVEREXPRESSION	**2h**	**6h**	**12h**
GO:0000087_M_phase_of_mitotic_cell_cycle			7/121 (0.0248)
GO:0007067_mitosis			7/119 (0.0258)